Supporting Information

Metallic Nanostructures via Static Plowing Lithography

Lon A. Porter, Jr., Alexander E. Ribbe, and Jillian M. Buriak*

[*] Prof. Jillian M. Buriak, Lon A. Porter, Jr., and Dr. Alexander E. Ribbe
Department of Chemistry, 1393 Brown Laboratories, Purdue University, West Lafayette, IN 47907-1393
Fax: (+1) 765-494-5302
E-mail: buriak@purdue.edu

Experimental Supplement

Materials. The following reagents were purchased from the indicated suppliers and used without modification: n-type (Sb-doped, 7 - 23 Ω·cm), p-type (Ga-doped, 0.004 - 0.020 Ω·cm) and intrinsic crystalline germanium wafers (Waferworld, (111) orientation), $HAuCl_4 \cdot 3H_2O$ (99.9%, Aldrich), $Cu(NO_3)_2$ (99%, Aldrich). Shipley 1805 series photoresist and Thinner P were obtained from MicroChem Corporation. Absolute ethanol was purchased from Pharmco Products Inc. Distilled water (18 MΩ) was purified using a Millipore (Barnstead) system. Optima grade pentane and tetrahydrofuran (THF) were purchased from Fisher. All other solvents and materials were obtained from commercial sources and used without modification.

Instrumentation

Atomic Force Microscopy (AFM). A Veeco Instruments, Nanoscope III™ scanning probe microscope was utilized in intermittent contact (tapping) mode operation for imaging of all nano/microstructures. Noncontact Si (MikroMasch, NSC15/50) tips with a resonance frequency of ~340 KHz were employed with a scan rate of 1-4 μm/s. The line widths of all structures are reported for full width at half max of the section profile plots (FWHM). While the height (z-axis) of a solid sample, such as gold, is usually accurate, the width of the observed line is widened due to convolution artifacts, a well known issue in scanning tunneling microscopy (STM) [Chicon, R.; Ortuno, M.; Abellan, J. *Surf Sci.* **1987**, *181*, 107.] and AFM [Villarubbia, J. S. *J. Res. Natl. Inst. Stand. Technol.* **1997**, *102*, 425.], which causes the x,y-dimensions of sample features to appear larger as they are in reality when their dimensions are in the range of the tip-curvature. All of the images presented in this work are presented without modification via deconvolution filters.

Scanning Electron Microscopy (SEM) and X-Ray Energy Dispersive Spectroscopy (EDS). In order to perform structural and qualitative analysis, SEM and EDS were employed with a JEOL JSM-35 CF. Both were acquired utilizing an accelerating voltage of 25 kV. EDS spectra were acquired at approximately 1500 cps and 15% detector deadtime.

Optical Ellipsometry. A Gaertner L116S, variable angle stokes ellipsometer (Azzam, R. M. A. *Thin Solid Films* **1993**, *234*, 371.) was utilized in determining applied resist layer thickness. Data was acquired with a He-Ne laser operating at 632.8 nm and incidence angle of 70°. The optical constants were obtained for bare Ge(111) after degreasing in acetone and methanol. The applied Shipley 1805 resist thicknesses were calculated assuming a refractive index of 1.64, supplied by MicroChem, Corporation.

Electrical Measurements. Metallic nano/microstructures were fabricated onto an undoped Ge(111) substrate and silver contacts were applied with conductive silver paint (Ted Pella, Inc.). The silver paint was applied with a glass capillary tube, with the aid of an optical microscope. Resistance measurements were conducted with a Keithley 4200 driven probe station.

Patterning Procedure: Static Plowing Lithography

Substrate Preparation. The Ge(111) substrates were cut into 1.0 × 1.0 cm squares and a simple "X" mark was scribed onto the center of the substrate, utilizing a fine point diamond scriber (Ted Pella, Inc.) with very light applied pressure. This mark served as a simple alignment mark for facilitating the relocation of fabricated nanostructures for imaging via SEM and AFM. The substrates were finally degreased by immersion into 4 successive baths of each of the following solvents: acetone, methanol, and deionized water. An additional soak in the above solvents was carried out with sonication for 2 min. The samples were subsequently blown dry with a stream of nitrogen.

Resist Application. A degreased 1 cm^2 Ge(111) wafer fragment was secured onto the vacuum chuck of a Speedline Technologies P6708 spin coater. The sample was practice spun at 2000 rpm for 30 s to assure proper centering. In order to obtain a sufficiently thin resist layer, the resist was diluted with propylene glycol monomethyl ether acetate (Shipley Thinner P). Approximately 0.1 mL of the thinned resist (1:15, Shipley 1805:Thinner P) was applied to the substrate and spun on at 2000 rpm for 30 s, followed by a 60 s bake at 95°C in a convection oven. This resulted in a 20 nm ± 2 nm resist layer, as determined via optical ellipsometry and collaborated utilizing atomic force microscopy. Resist layer thickness could be tailored through the careful modulation of resist dilution. Particulate matter in the laboratory environment that found its way to the substrate surface produced pinhole defects in the resist layer. Samples proved difficult to keep free of particulate matter and the use of a cleanroom facility is highly recommended.

Resist Plowing via AFM Static Plowing. A scanning probe microscope (Nanoscope III, Veeco Instruments) was used as a lithography tool for writing and tapping mode atomic force microscopy for imaging. The resist-coated sample was adhered onto a stainless steel specimen disc (Ted Pella, Inc.) with a small square of carbon tape and secured onto the tube scanner. With the aid of an overhead mounted optical microscope, the AFM tip was aligned such that features were plowed within a given distance of the microscribe alignment marks. An oxide sharpened (tip radius of curvature <10 nm), silicon tip (MikroMasch, NSC-15) with a high spring constant (40 N/m) was utilized for both plowing through the thin resist and imaging of the resulting furrow. Static plowing was accomplished in contact mode operation, where the tip was scanned across the sample surface with a constant force (3-5 μN). This setpoint proved sufficient to displace the soft polymer resist, thereby exposing the Ge(111) surface as scanning progressed. Furthermore, this force did not result in any observable damage to the underlying semiconductor substrate. Increasing the force applied to the tip beyond ~5 μN, however, resulted in 1-2 nm indentations into the germanium surface (Figure SI-3). The resulting furrows were immediately characterized via atomic force microscopy, employing the same tip, by switching to intermittent contact, or tapping mode, operation for imaging. Tips were observed to remain sharp following static plowing, foregoing the need to exchange tips, and no residual resist material was observed to adhere to the tip surface. Continuous furrows, flanked by displaced resist were reproducibly obtained at scanning speeds of nearly 100 μm/s, with lengths in hundreds of microns, restricted only by the range of the available AFM scanner. Vector scan operation allows for the AFM tip to be driven along paths of arbitrary length scales at predefined angles, while also providing for control over z-axis displacement and applied force. Utilizing the NanoScript™ software (Veeco Instruments), a general programming script provided access to a myriad of customized scan profiles. As a consequence of open-loop instrument, such as the Nanoscope III, some drift was observed in the resist furrows. Scan rates were highly dependant upon the desired geometry complexity and scale. For example, complex letters and designs required slower scan speeds of nearly 1-5 μm/s, whereas solid shapes and long lines were fabricated at speeds in excess of 100 μm/s.

Deposition onto Patterned Surfaces. The entire substrate was carefully removed from the AFM specimen disc and immersed into a dilute, aqueous solution of $HAuCl_4$ or $Cu(NO_3)_2$, depending on the metal species of interest. Exposed domains of the Ge(111) result in intimate contact between the semiconductor bulk and the metal salt solution, whereas the residual resist concealed the majority of the wafer surface from the aqueous plating solution. Metal deposition onto the exposed Ge(111) proceeds via galvanic displacement in the absence of fluoride, pH buffers, complexing agents, or external reducing agents, as previously demonstrated in earlier work. Following electroless deposition, the substrate was removed from the plating solution and washed thoroughly with water, ethanol, tetrahydrofuran, and pentane. This proved to wash away any residual plating solution as well as stripping the remaining resist material. The samples were finally blown dry utilizing a high-pressure stream of nitrogen.

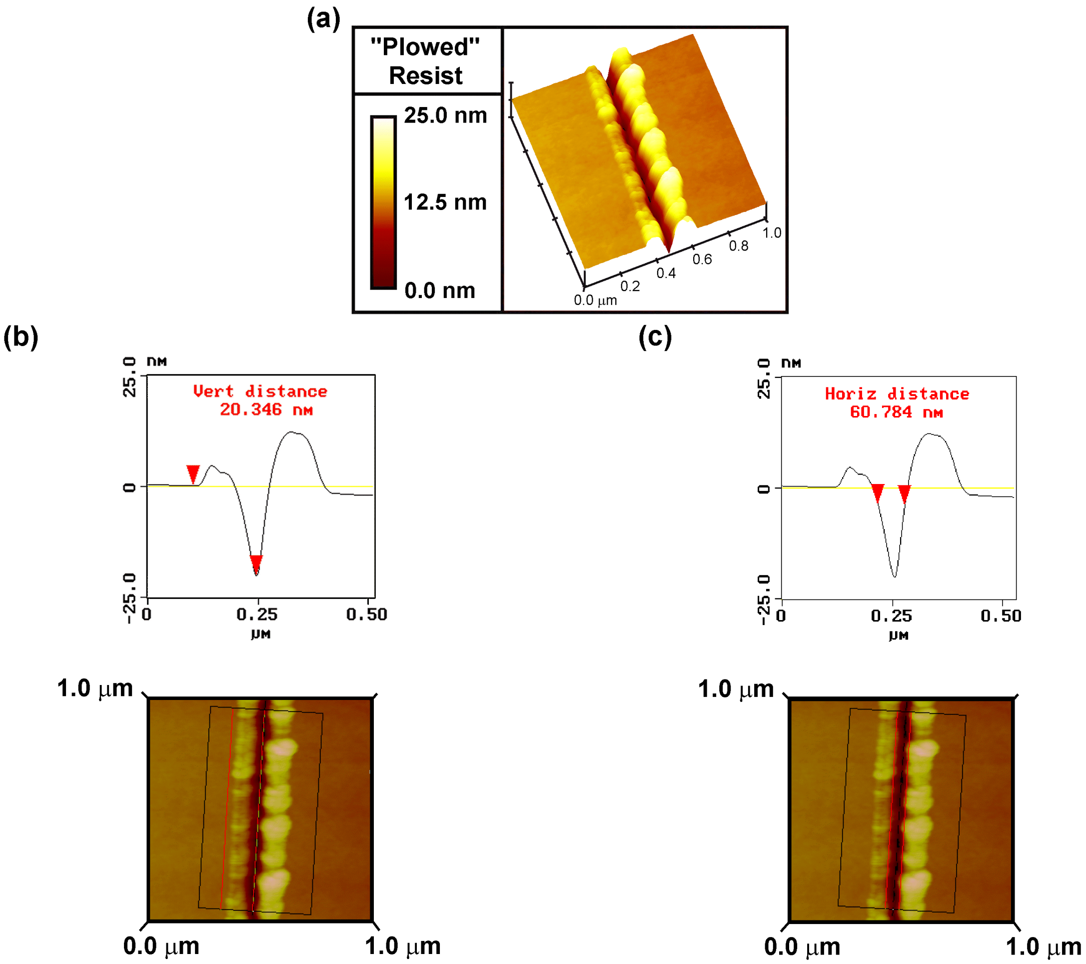

Figure SI-1. Intermittent contact (Tapping) mode atomic force micrographs illustrating a resist furrow produced by static plowing (a) along with the corresponding section plots illustrating the depth (b) and width (c) of the furrow.

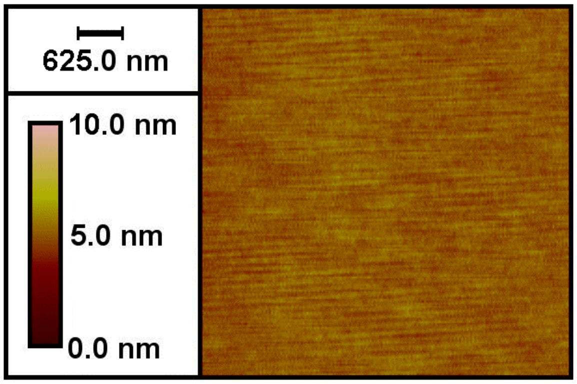

Figure SI-2. Intermittent contact (Tapping) mode atomic force micrograph showing the resist surface prior to plowing lithography.

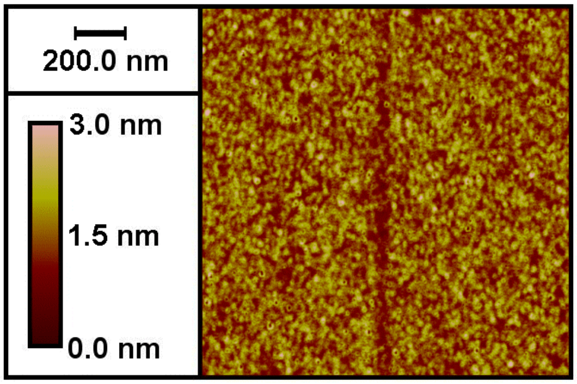

Figure SI-3. Intermittent contact (Tapping) mode atomic force micrograph showing the indentation into the Ge(111) surface resulting from static plowing though the ploymer resist with excessive force applied to the tip.

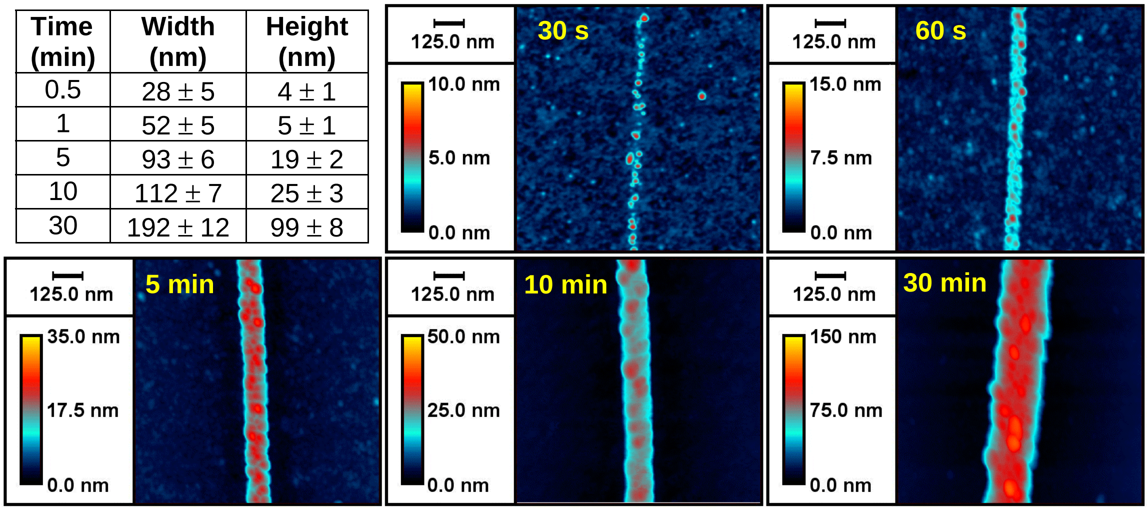

Time (min)	Width (nm)	Height (nm)
0.5	28 ± 5	4 ± 1
1	52 ± 5	5 ± 1
5	93 ± 6	19 ± 2
10	112 ± 7	25 ± 3
30	192 ± 12	99 ± 8

Figure SI-4. Intermittent contact (Tapping) mode atomic force micrographs illustrating gold nanostructures on Ge(111) resulting from increasing immersion times in 25 μM $HAuCl_{4(aq)}$ at 25°C, following resist removal. Grain size is observed to increase with longer plating times.

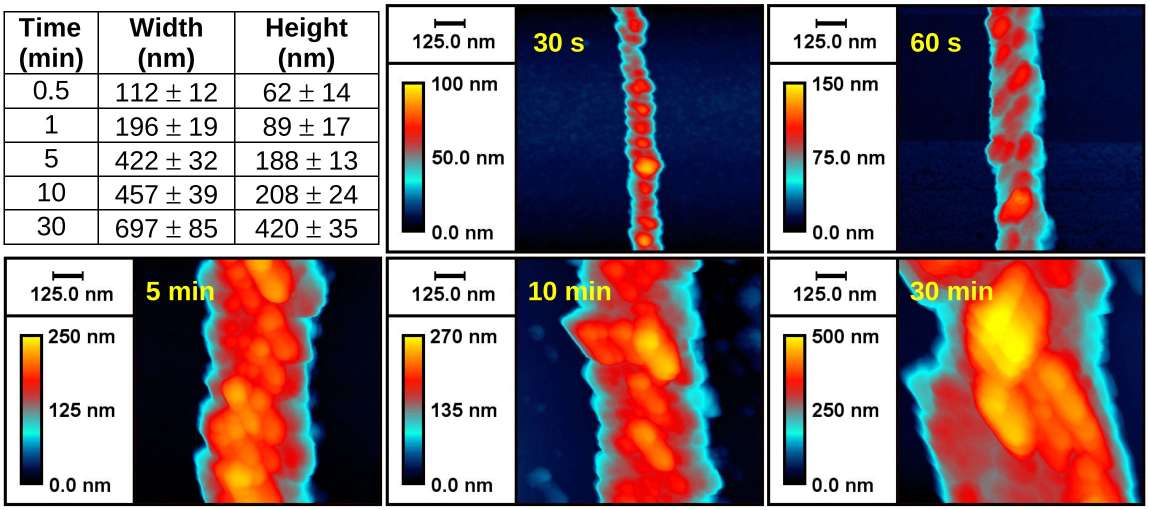

Time (min)	Width (nm)	Height (nm)
0.5	112 ± 12	62 ± 14
1	196 ± 19	89 ± 17
5	422 ± 32	188 ± 13
10	457 ± 39	208 ± 24
30	697 ± 85	420 ± 35

Figure SI-5. Intermittent contact (Tapping) mode atomic force micrographs illustrating gold nano/microstructures on Ge(111) resulting from increasing immersion times in 50 μM $HAuCl_{4(aq)}$ at 25°C, following resist removal. The surface topography of these structures is more clearly shown in the corresponding scanning electron micrographs, show in Figure SI-10.

Time (min)	Width (nm)	Height (nm)
0.5	274 ± 16	128 ± 16
1	442 ± 43	241 ± 32
5	711 ± 108	407 ± 56
10	1105 ± 188	637 ± 191
30	1355 ± 359	839 ± 196

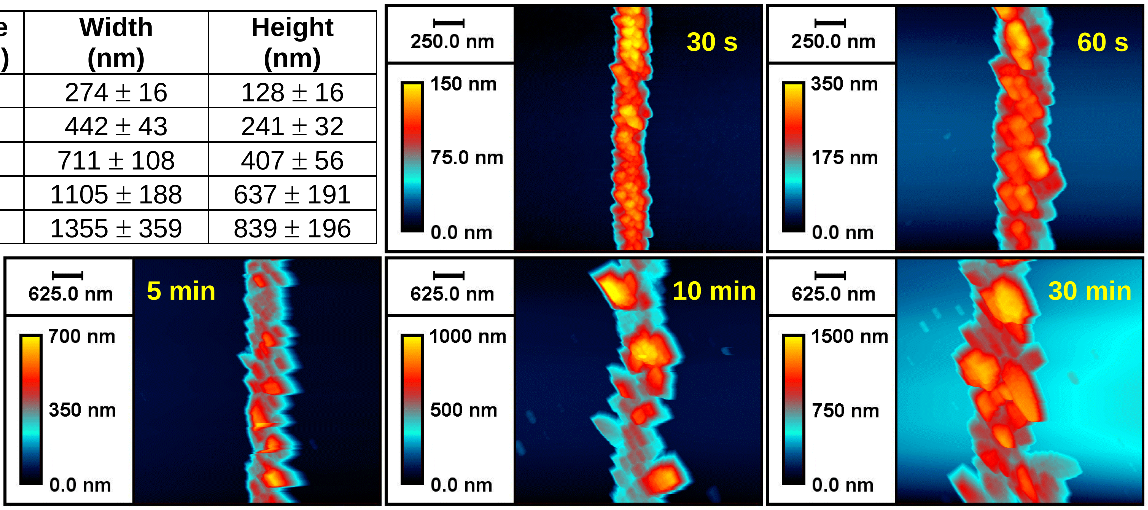

Figure SI-6. Intermittent contact (Tapping) mode atomic force micrographs illustrating gold nano/microstructures on Ge(111) resulting from increasing immersion times in 100 μM $HAuCl_{4(aq)}$ at 25°C, following resist removal.

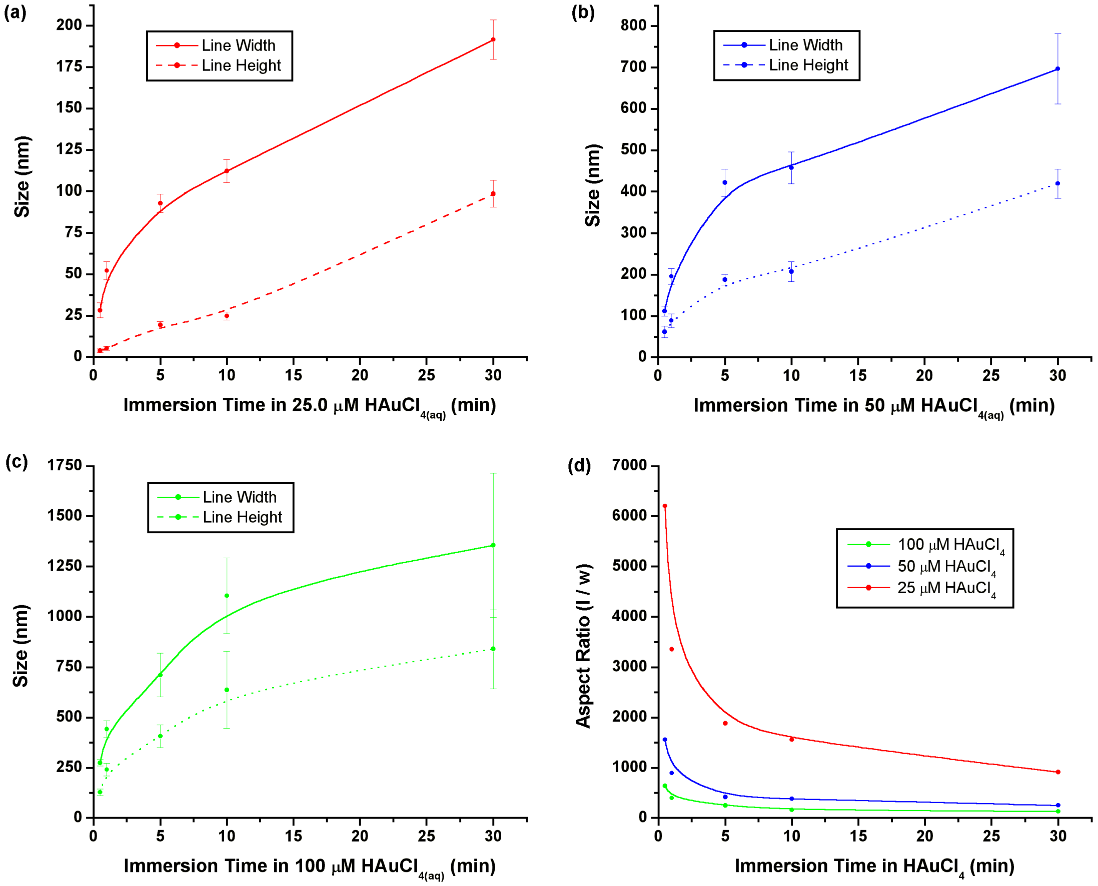

Figure SI-7. Effect of immersion time on gold nano/microstructure line width (solid line) and height (broken line) patterned via static plowing lithography on Ge(111) from 25 μM (a), 50 μM (b), and 100 μM (c) $HAuCl_4$ at 25°C. These 185 μm long structures were observed to yield extremely high aspect ratios, as prepared from 25 μM (red), 50 μM (blue), and 100 μm (green) solutions of $HAuCl_4$ at 25°C.

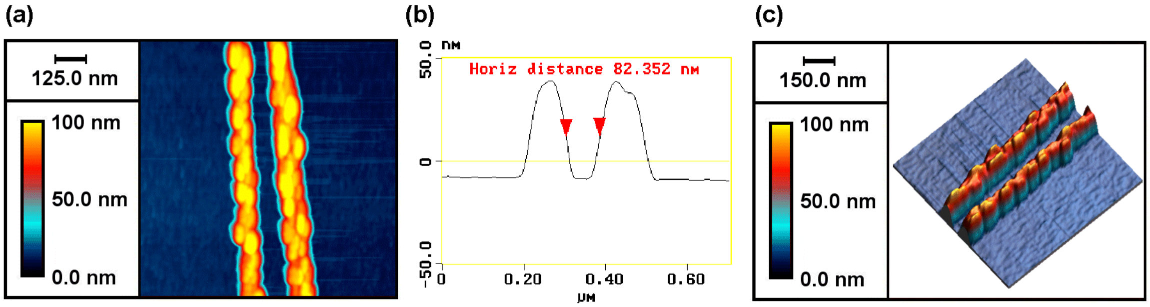

Figure SI-8. Intermittent contact (Tapping) mode atomic force micrographs illustrating two gold nanostructures fabricated parallel to each other, with ~85 nm spacing (a) prepared from a 30 s immersion in 50 µM $HAuCl_{4(aq)}$ at 25°C, following resist removal. The corresponding section plot (b) and 3D representation (c).

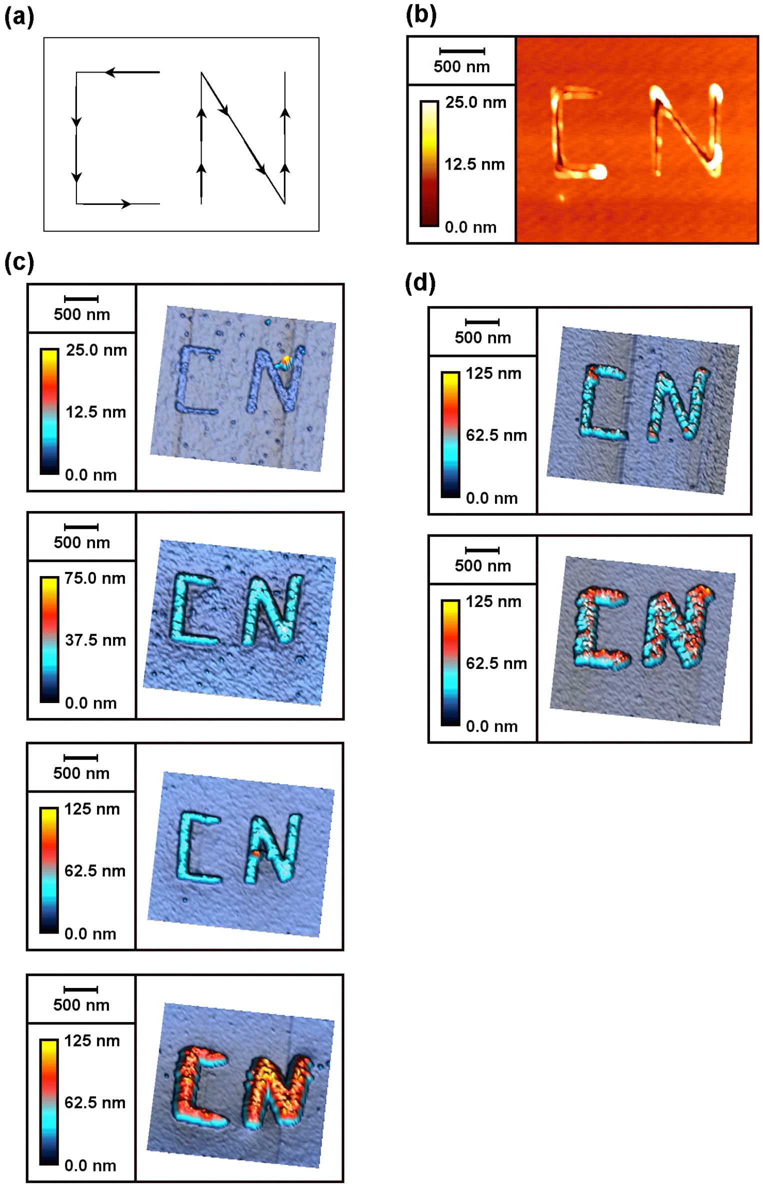

Figure SI-9. Employed vector pattern (a) and intermittent contact (Tapping) mode atomic force micrographs illustrating a series of resist furrows (CN - Chemical Nanotechnology) produced by static plowing (b) and the gold nanostructures on Ge(111) resulting from a 1, 5, 10, and 30 min immersion (top to bottom) in 25 μM $HAuCl_{4(aq)}$ at 25°C, following resist removal (c). The gold nanostructures on Ge(111) resulting from a 30 s and 1 min immersion (top to bottom) in 50 μM $HAuCl_{4(aq)}$ at 25°C, following resist removal (c).

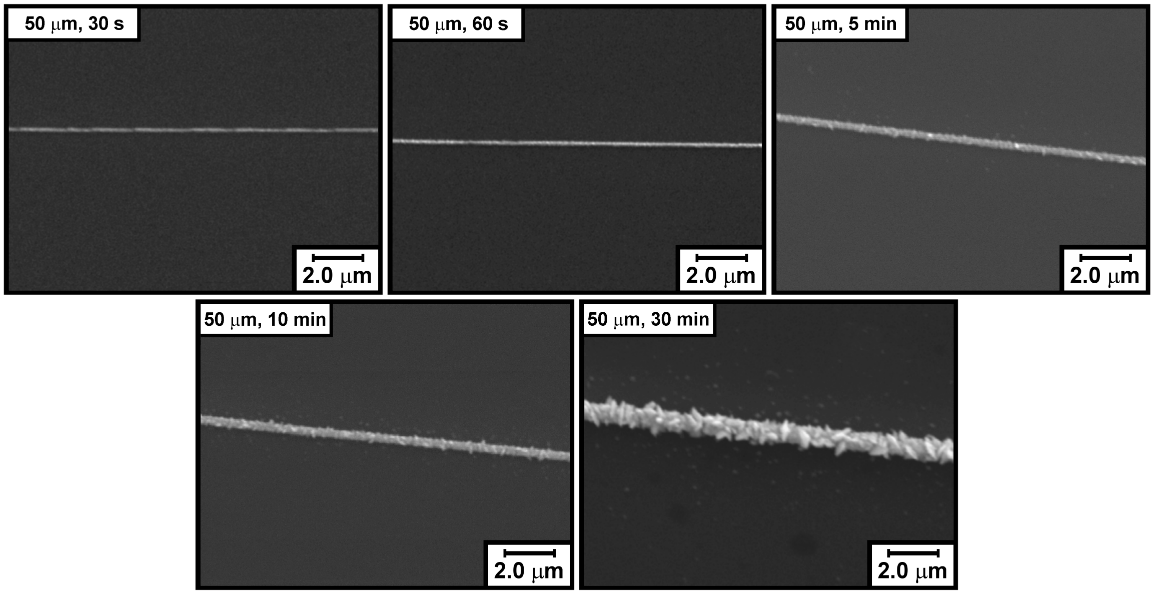

Figure Si-10. Scanning electron micrographs of gold nano/microstructures on Ge(111) resulting from increasing immersion times in 50 μM $HAuCl_{4(aq)}$ at 25°C, following resist removal.

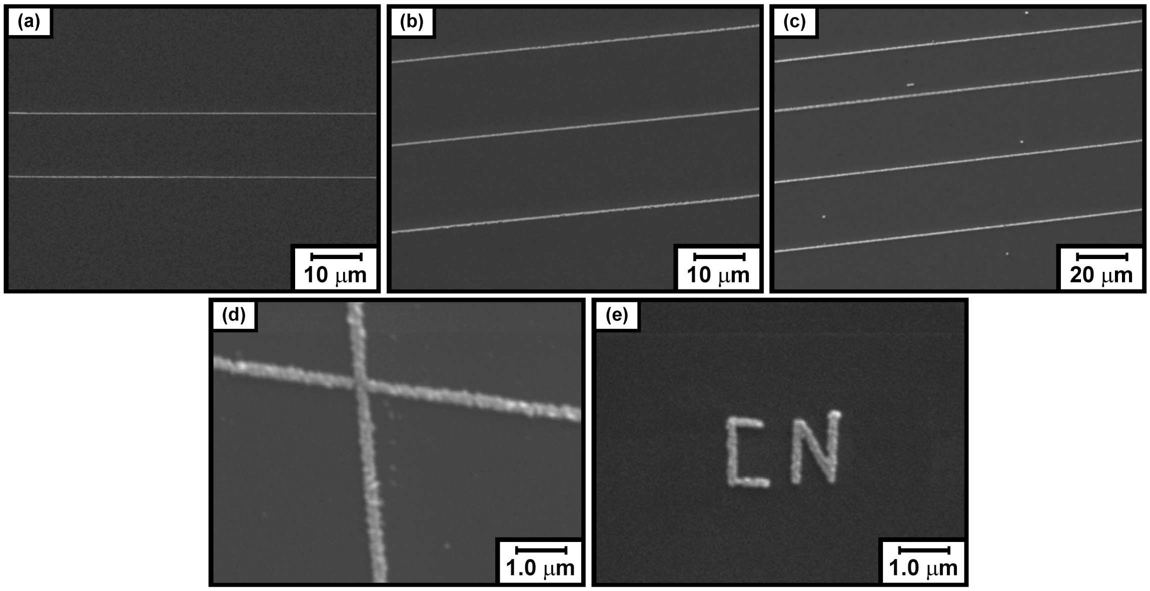

Figure SI-11. Scanning electron micrographs of parallel gold nano/microstructures on Ge(111) resulting from 1 (a), 10 (b), and 30 min (c) immersion times in 50 μM $HAuCl_{4(aq)}$ at 25°C, following resist removal. A set of intersecting gold structures (d) and a pair of letters (e) are shown on Ge(111) prepared from 5 min and 1 min immersion times, respectively, in 50 μM $HAuCl_{4(aq)}$ at 25°C, following resist removal.

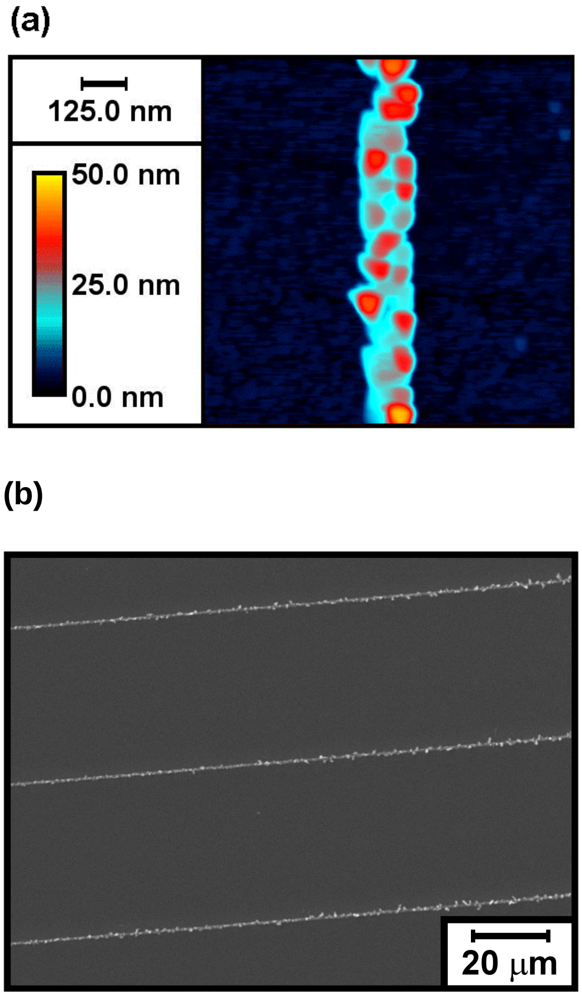

Figure SI-12. Intermittent contact (Tapping) mode atomic force micrograph illustrating a copper nanostructure (a) prepared from a 30 s immersion in 50 μM $Cu(NO_3)_2$ and scanning electron micrograph showing paralled copper nanostructures (b) prepared from a 30 min immersion in 50 μM $Cu(NO_3)_2$.

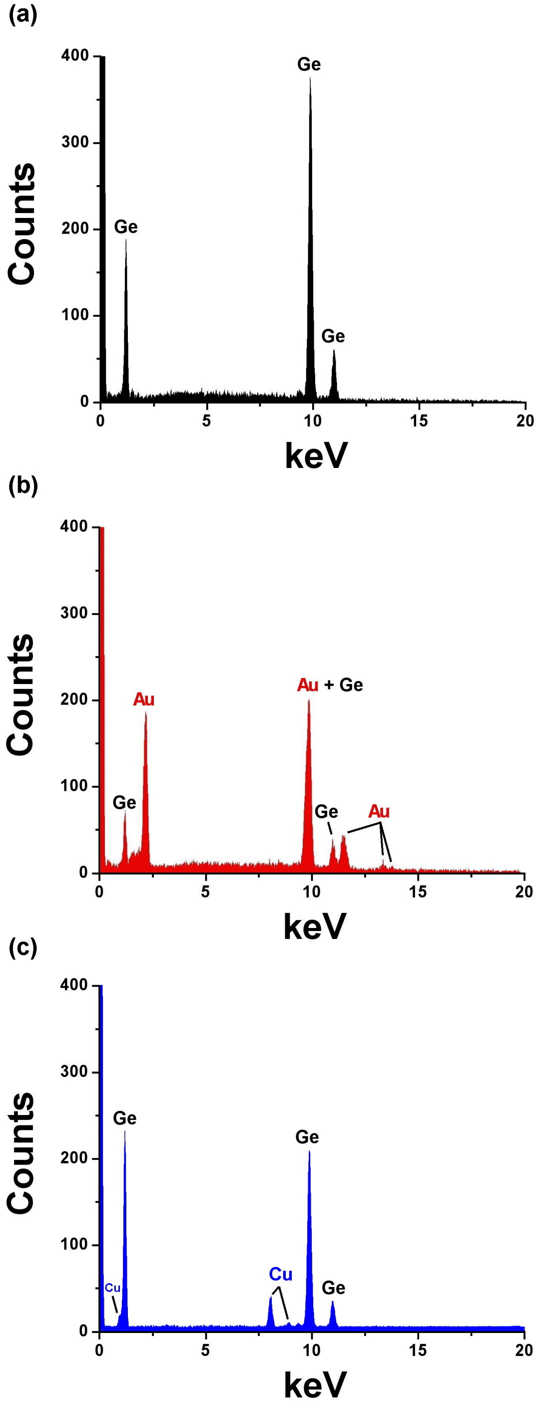

Figure SI-13. X-ray energy dispersive spectra of bare Ge(111) (a), gold nano/microstructures on Ge(111) resulting from a 30 min immersion in 50 μM $HAuCl_{4(aq)}$ (b) and copper nano/microstructures on Ge(111) resulting from a 30 min immersion in 50 μM $Cu(NO_3)_{2(aq)}$ (c) at 25°C, following resist removal.

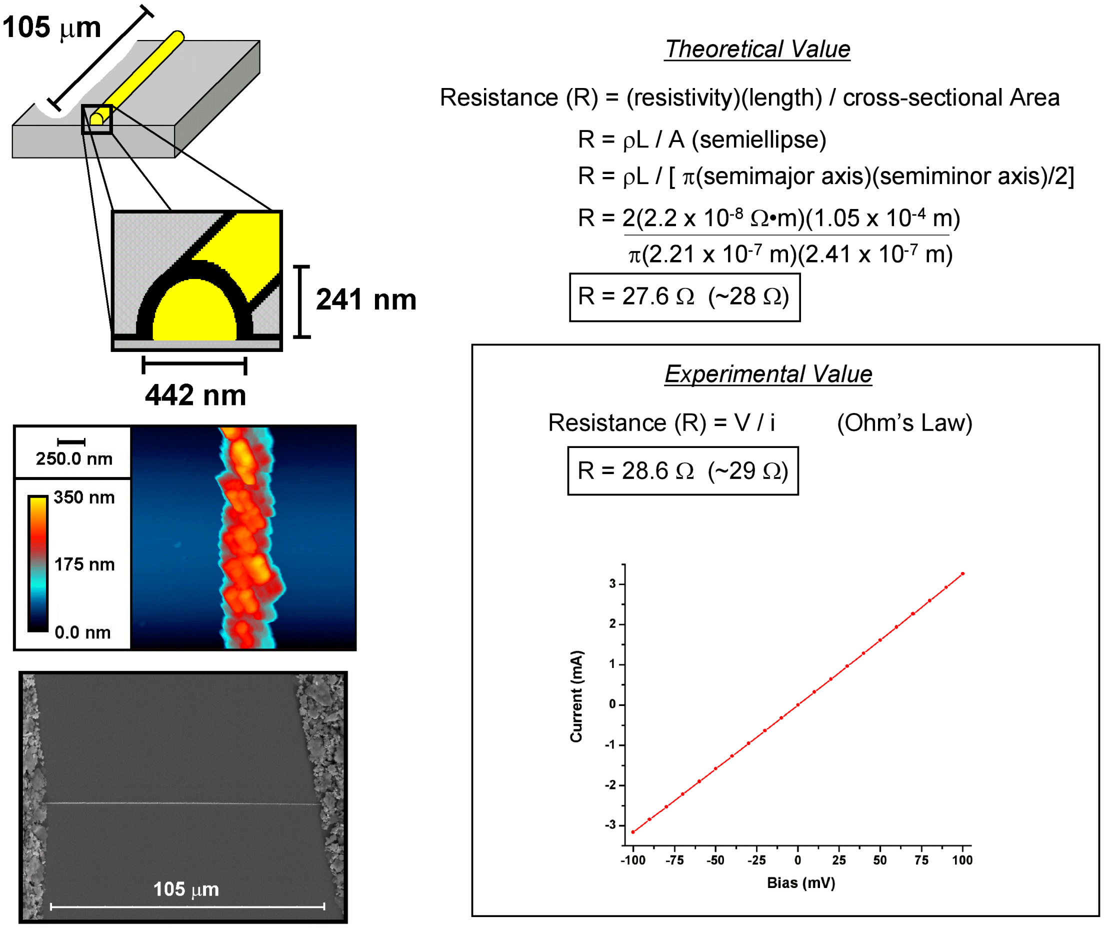

Theoretical Value

Resistance (R) = (resistivity)(length) / cross-sectional Area

$R = \rho L / A$ (semiellipse)

$R = \rho L / [\ \pi(\text{semimajor axis})(\text{semiminor axis})/2]$

$$R = \frac{2(2.2 \times 10^{-8}\ \Omega\bullet\text{m})(1.05 \times 10^{-4}\ \text{m})}{\pi(2.21 \times 10^{-7}\ \text{m})(2.41 \times 10^{-7}\ \text{m})}$$

$\boxed{R = 27.6\ \Omega\ \ (\sim 28\ \Omega)}$

Experimental Value

Resistance (R) = V / i (Ohm's Law)

$\boxed{R = 28.6\ \Omega\ \ (\sim 29\ \Omega)}$

Figure SI-14. Data, micrographs, and calculations more fully explaining electrical testing results and calculations.

For background concerning use of this silver paint procedure, see: Walter, E. C.; Favier, F.; Penner, R. M. *Anal. Chem*. **2002**, *74*, 1546.